Available online at www.sciencedirect.com
ScienceDirect
International Communications in Heat and Mass Transfer 35 (2008) 446–457
International Communications in HEAT and MASS TRANSFER
www.elsevier.com/locate/ichmt

An evaluation on thermal performance of CPC solar collector ☆

Yong Kim [a], GuiYoung Han [b], Taebeom Seo [c,*]

[a] Department of Mechanical Engineering, Inha University, Inchon, South Korea
[b] Department of Chemical Engineering, Sungkyunkwan University, Suwon, South Korea
[c] Department of Mechanical Engineering, Inha University, 253, Yonghyundong, Namgu, Inchon, 402-751, South Korea

Available online 26 November 2007

Abstract

The main objective of this work is the investigation and improvement of thermal performance of evacuated CPC (Compound Parabolic Concentrator) solar collector with a cylindrical absorber. Modified types of this solar collector are always combined with the evacuated glass envelop or tracking system. The conventional stationary CPC solar collector has been compared with the single axis tracking CPC solar collector in outlet temperature, net heat flux onto the absorber and thermal efficiency. Numerical model has been analyzed based on the irradiation determined actually and the results have been calculated to predict the thermal efficiency. Based on the comparison of the measured and calculated results, it is concluded that the numerical model can accurately estimate the performance of solar collectors. The result shows the thermal efficiency of the tracking CPC solar collector is more stable and about 14.9% higher than that of the stationary CPC solar collector.

Keywords: Thermal performance; Evacuated CPC solar collector; Sun tracking; Water heating

1. Introduction

As medium-temperature solar collectors, the Compound Parabolic Concentrator (CPC) solar collector has a lot of merits including both the concentrating collector and the flat plate collector[1]. CPC solar collector can not only gather the solar beam to the receiver with a reflector/refractor but also utilize the beam and diffuse solar irradiation like a flat plate solar collector. Therefore, CPC solar collectors are always efficient than typical flat plate solar collector. Ronnelid's research referred that with the same testing condition, the heat loss coefficients of a flat plate solar collector could be up to 32% more than a prototype CPC solar collector [2]. Tchinda theoretically investigated the thermal performance of CPC with flat absorber with various dimensions. The results showed that when the tube of relatively long length is used as the absorber of the solar collector or

☆ Communicated by W.J. Minkowycz.
* Corresponding author.
E-mail address: seotb@inha.ac.kr (T. Seo).

0735-1933/$ - see front matter © 2007 Elsevier Ltd. All rights reserved.
doi:10.1016/j.icheatmasstransfer.2007.09.007

Nomenclature

R	Radius (mm)
d	Diameter (mm)
A	Area (m^2)
V	Velocity (m/s)
$\dot{m}$	Mass flow rate (kg/s)
P_g	Gauge pressure (Pa)
c_p	Specific heat (kJ/kg K)
Q	Heat flux (W/m^2)
G	Insolation (W/m^2)
T	Temperature (K)
D	Copper tube outer diameter (mm)
k_T	Clearness index
I	Solar irradiation (J/m^2)
I_o	Extraterrestrial solar irradiation (J/m^2)
I_d	Diffuse solar irradiation (J/m^2)

Greek letters

σ	Stefan–Boltzmann constant
ε	Emittance
η	Efficiency

Subscripts

c	Copper
g	Glass
i	Inner or inlet
o	Outer or outlet
w	Water
loss	Heat loss
r	Reflector

the inlet temperature of the cooling fluid increases, the outlet temperature of the cooling fluid and the daily efficiency decrease [3]. Also, researches presented that CPC solar collectors combined with doubled-layered evacuate glass tube are employed in many solar systems because the conductive and convective heat losses can be eliminated by the vacuum space [4]. Two-axes concentrator can obtain higher geometric concentration ratio than one-axis concentrator, however, exorbitant charge and the troubles of maintaining the equipments make it not so cost effective [5 6 7]. There are also lots of literatures relating to the comparison of stationary and tracking solar collectors. Abdul–Jabbar made an experiment on the effect of two-axis tracking CPC solar collector deducing that the tracking solar collector showed a better performance of up to 75% compared with identical fixed solar collector [1]. Gandhidasan and Satcunana presented their works about theoretical comparative study between full-tracking, semi-tracking and stationary solar collector [8].

In this paper, the one-axis tracking system, which is relatively cheap and easy to set up, is taken. As the CPC with internal-reflector is more available for easy maintenance than that with external-reflector, the former is used for this experiment. The double-layered glass evacuated tube can not only prevent the performance deterioration of the reflector caused by the external condition like as the dust but also

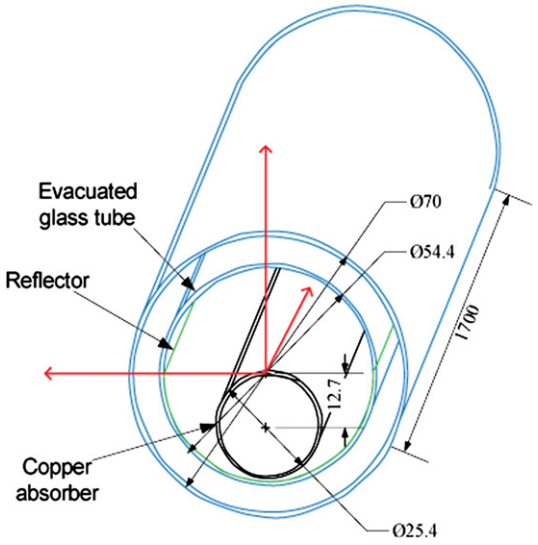

Fig. 1. Main dimensions of CPC solar collector.

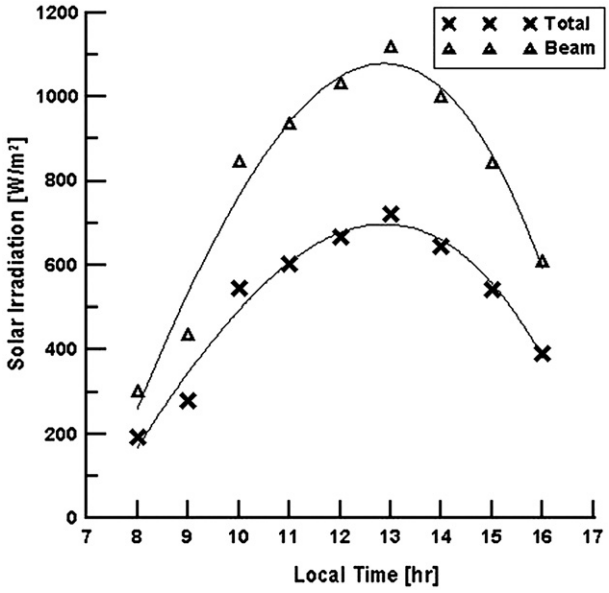

Fig. 2. Beam and total solar irradiation with the local time.

minimize the convective heat loss (natural convection heat loss+forced convection heat loss) [9,10]. Mechanical tracking system has been used to adjust the orientation of the solar collector, which makes the solar collector track the sun. In this way, the incident angle of beam irradiation can be always

Fig. 3. Ray-tracing results with incidence angle of (a) 0°, (b) 30°, (c) 60°. (red: the incident rays, green: the reflected rays to the absorber and the transmission rays, blue: the refracted and reflected rays to the ambient). (For interpretation of the references to colour in this figure legend, the reader is referred to the web version of this article.)

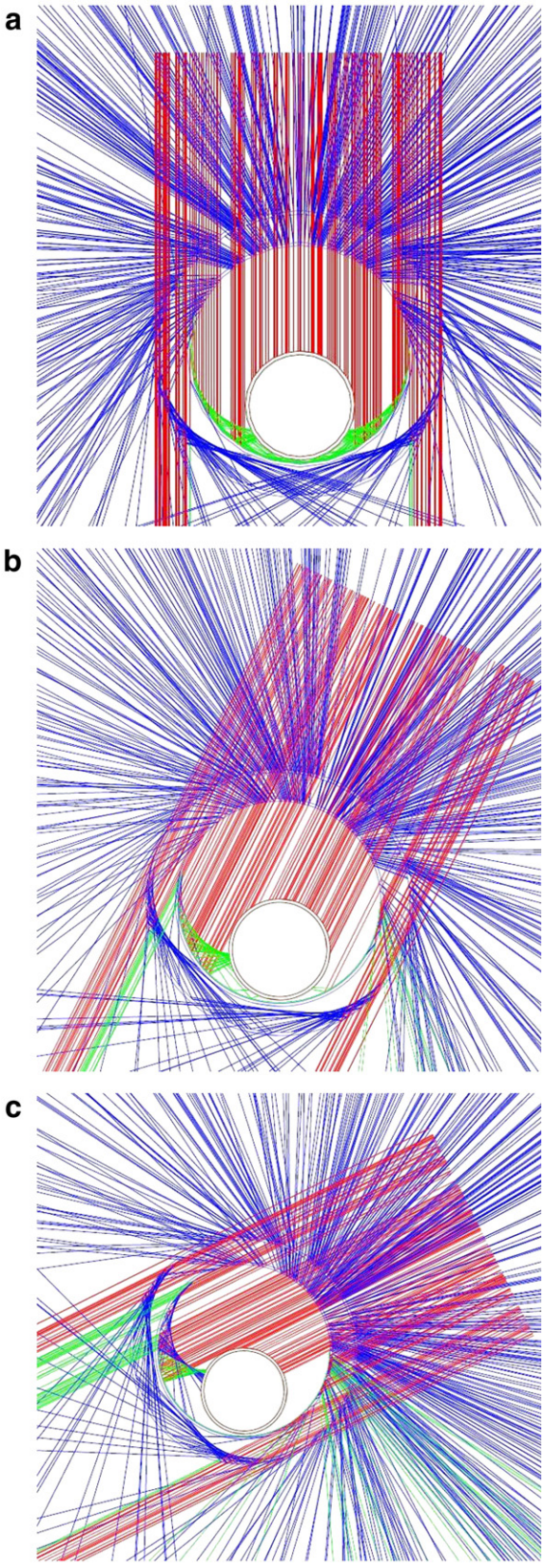
a
b
c

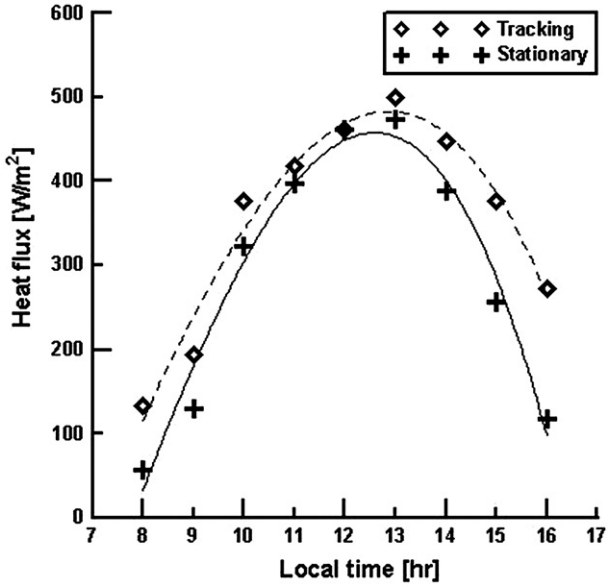

Fig. 4. Heat flux absorbed on copper tube with local time.

adjusted to 0°. In this paper, both beam and diffuse irradiation are taken into account. The CPC solar collector has been designed, constructed and tested in Incheon(37°30′N, 126°38′E), Korea. The main objective of the current work is to numerically and experimentally investigate the performance of the stationary and tracking CPC solar collectors and to compare two system performances. These numerical calculation and experimental results are analyzed and discussed in detail for further researches such as CPC solar collector design or performance evaluations.

2. Numerical analysis

A simplified numerical model has been set up to simulate the experimental apparatus. Main dimensions are shown in Fig. 1. The reflector is attached onto the inner glass tube. The thickness of the reflector, outer glass tube, inner glass tube, copper tube is 0.5 mm, 1.8 mm, 1.6 mm and 1.8 mm, respectively. In order to investigate the heat flux with the incidence angle, the ray-tracing code TRACE PRO [11] is

Table 1
Boundary conditions

Position	Condition
Inlet ($z=0$, $r<d_{ci}/2$)	$T_i=20.05$ °C, $u=0$, $v=0$, $w=V/A_c$ ($V=5.56\times10^{-6}$ m^3/s)
Outlet ($z=1.7$ m, $d_{c,o}/2<r<d_{g,i}/2$)	$P_g=0$
Wall ($r=d_{c,i}/2$, $d_{c,o}/2$, $d_{g,i}/2$)	Velocity: $u=0$, $v=0$, $w=0$
On the copper tube surface ($r=d_{co}/2$)	$q=q_0$ (constant)
Radiative heat loss of copper tube, glass tube and aluminum reflector	$\text{At } r=d_{co}/2,\quad q_{c,loss}=\varepsilon_c\sigma\left(T_c^4-T_s^4\right)$ $\text{At } r=d_{go}/2,\quad q_{g,loss}=\varepsilon_g\sigma\left(T_g^4-T_s^4\right)$ $\text{At } r=d_{go}/2,\quad q_{r,loss}=\varepsilon_r\sigma\left(T_r^4-T_s^4\right)$

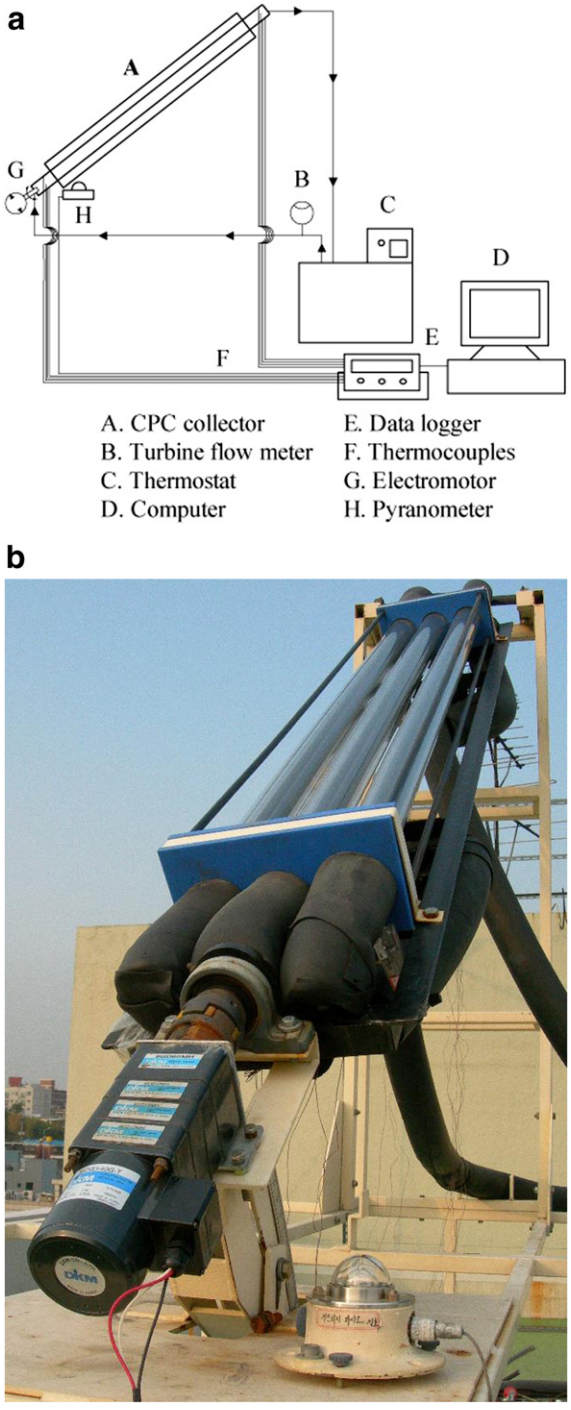

Fig. 5. Experimental apparatus.

used. The interval of the numerical model has been set to 15° for the variation of the incident angle which is from −60° to 60° by assuming the normal incidence according with the negative direction of axis y. The heat flux absorbed on each surface of the solar collector component is analyzed numerically with this commercial code.

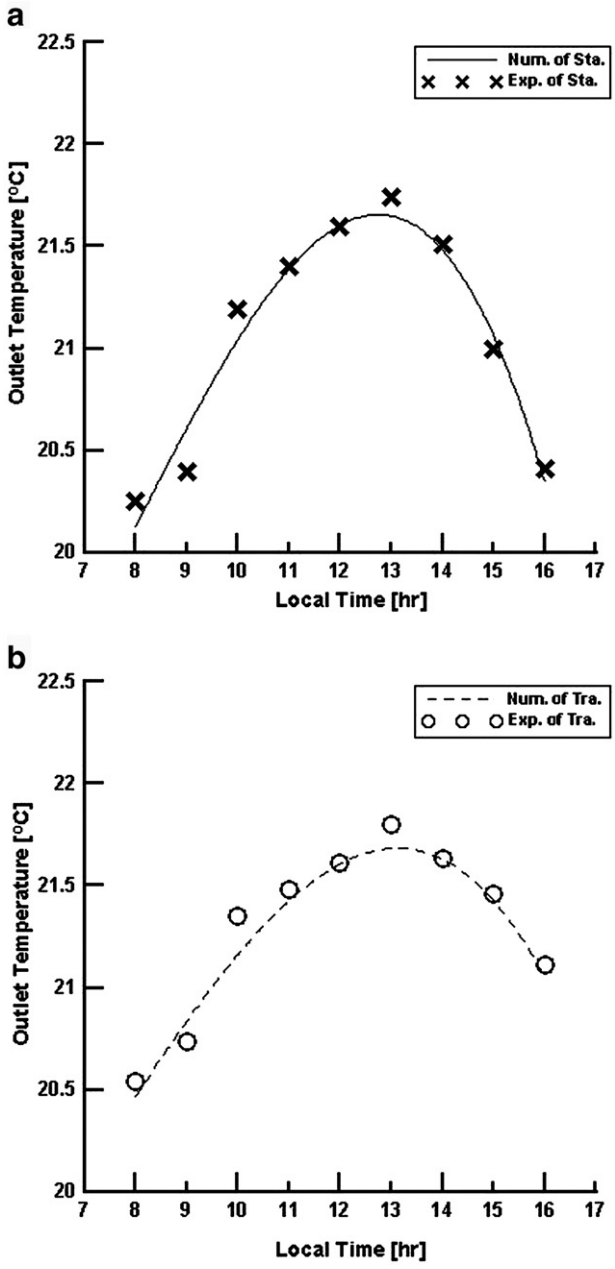

Fig. 6. Outlet temperature of (a) stationary and (b) one-axis tracking CPC solar collector with local time.

The total irradiation data are monitored and recorded with a pyranometer (EPPLEY PSP 213731-3) during several days. In order to calculate the diffuse irradiation and the beam irradiation, the hourly clearness index [12] is used as follows;

$$k_T = \frac{I}{I_o} \tag{1}$$

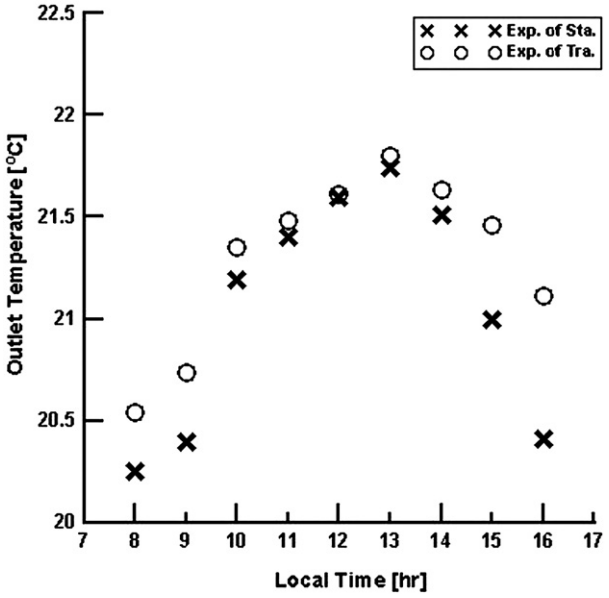

Fig. 7. Outlet temperature of both stationary and tracking collector with local time.

where,

I solar irradiation,
I_o extraterrestrial solar irradiation

$$\frac{I_d}{I} = 0.9511 - 0.1604k_T + 4.388k_T^2 - 16.638k_T^3 + 12.336k_T^4 \quad (2)$$

(for $0.22 < k_T \leq 0.80$)

where, I_d = diffuse component.

The diffuse irradiation and the beam irradiation are calculated by Eq. (1) and Eq.(2), and the results are shown in Fig. 2. The hourly clearness index [12] (k_T) is assumed as 0.64 in this study [13]. The total irradiation, as well as the beam component goes on increasing until about 13 in the afternoon. The beam component also describes a similar trend as the total irradiation.

A ray-trace projection of 100,000 rays apart from fixed positions is carried out for the two dimensional models of both stationary and tracking CPC solar collectors. The amounts of absorbed heat flux are analyzed with the incident angle and the beam intensity. In Fig. 3, the ray tracing results of the stationary CPC solar collector show that the beam, which falls on the absorber, decreases obviously as the incidence angle increases. The increase of the incident rays which pass by the solar collector leads to an energy consumption to the ambient. This is also because the reflector blocks off some of the incident beam without normal incidence. On the other hand, the tracking CPC solar collector which always holds the normal incidence can maximize the absorbing heat flux. Radiative properties used for this study are predefined. The transmissivity and absorptivity of the glass tube are 0.91 and 0.018, respectively. The absorptivity of the copper tube is 0.93. The aluminum reflector has a reflectivity of 0.9.

Fig. 4 presents the absorbed heat fluxes of both stationary and tracking CPC solar collector based on the ray-tracing results with the measured irradiation. Both the stationary and the tracking CPC solar collector present a peak of absorbed energy at about 13 p.m. with its corresponding peak irradiation. It is also clear that the heat flux does not change as quickly as in the morning. The largest deviation of two collectors appears at 16 p.m. whereas the smallest deviation can be found at 12 a.m. from this graph.

The outlet temperatures of each CPC solar collector are calculated by a commercial FVM code. The water, which is chosen as the cooling fluid, flows inside the absorber tube as the laminar flow. The boundary conditions are shown in Table 1.

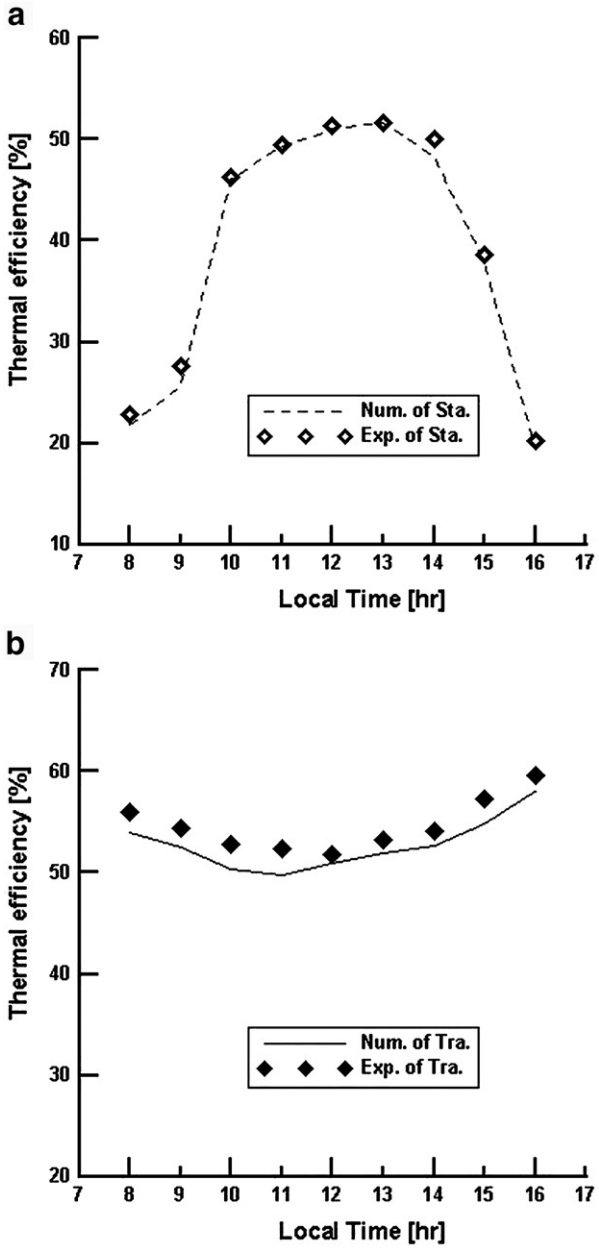

Fig. 8. Thermal efficiency of (a) the stationary and (b) tracking CPC collector with local time.

To simplify the calculations without losing accuracy significantly, some available assumptions are adopted. Each heat transfer process is served to be steady state. The convective heat loss coefficient from the glass envelope to the ambient is fixed at 2 W/m^2 K for all the numerical models. The radiative heat loss of the copper tube surface, the reflector surface and the glass tube surface are also taken into account. Although the incident heat flux is, in fact, not constant on absorber surface, it is assumed to be constant for this numerical model because the thermal conductivity of the absorber tube is very high.

3. Experimental setup and procedure

The experiment apparatus is shown in Fig. 5. The dimensions are completely same with the numerical model (Fig. 1). To evaluate the performance of the stationary and tracking CPC solar collectors, the irradiation, flow

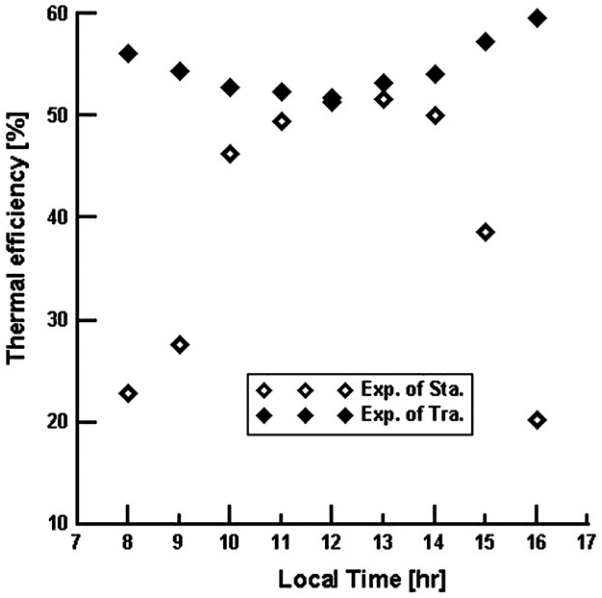

Fig. 9. Thermal efficiency of stationary and tracking collector with different time.

rate and temperatures are measured during several days with various irradiations. Both two solar collectors are installed and tested facing south. And the test sections are set at a tilt of from horizontal to the latitude of Incheon (37.5°) in this outdoor fieldwork. The tracking CPC solar collector is at an interval of 15°/h with the direction of anticlockwise round axis *z*. An electromotor controlled by frequency-adjustable converter is taken to drive the collectors.

In order to minimize the conductive and convective heat losses, glass tubes with the vacuum space pressure below 0.05 Pa are introduced to this experiment. The polished aluminum reflector and the copper absorber painted with dark black paint are mounted into each glass and three collectors are housed in a plastic manifold. Water is chosen as the cooling fluid because it has a quick temperature response and is one of the readily available fluids. This experiment is performed at the volume flow rate of 20 lpm for each tube. The volume flow rate is measured by a turbine flow meter. A thermostat which can adjust the inlet temperature is used to circulate the water. The direction of this water loop is denoted as the arrows shown in Fig. 5. The in-and outlet temperatures are measured using T-type copper-constantan thermocouples linked to a data logger (Agilent 34970A). The global irradiation is measured with a pyranometer. All

Table 2
Outlet temperature of stationary and one-axis tracking CPC solar collector with local time

Local Time	Stationary CPC solar collector			Tracking CPC solar collector		
	Num [°C]	Exp [°C]	Error [%]	Num [°C]	Exp [°C]	Error [%]
8	20.22	20.25	0.14	20.52	20.54	0.09
9	20.37	20.40	0.13	20.69	20.74	0.24
10	21.19	21.19	0.02	21.27	21.35	0.39
11	21.40	21.40	0.02	21.40	21.48	0.36
12	21.59	21.60	0.06	21.59	21.61	0.10
13	21.71	21.74	0.14	21.78	21.80	0.11
14	21.46	21.51	0.22	21.57	21.63	0.29
15	20.98	21.00	0.09	21.39	21.46	0.31
16	20.40	20.41	0.05	21.08	21.11	0.13

Table 3
Thermal efficiency of stationary and tracking CPC solar collector with local time [%]

Local Time	Stationary CPC solar collector			Tracking CPC solar collector		
	Num	Exp	Nup/Exp	Num	Exp	Nup/Exp
8	21.83	22.88	95.41	53.98	56.07	96.27
9	25.58	26.60	96.17	52.56	54.42	96.58
10	46.09	49.44	99.59	50.41	52.77	95.53
11	49.29	49.44	99.70	49.78	52.37	95.05
12	50.99	51.39	99.22	50.99	51.73	98.57
13	51.70	51.71	99.98	51.98	53.22	97.67
14	48.34	49.99	96.70	52.60	54.10	97.23
15	37.87	38.64	98.01	54.77	57.4	95.52
16	19.69	20.23	97.33	57.98	59.56	97.35

measured data are continuously monitored with an interval of 5 min. These data signals are then recorded and managed by a computer.

4. Results and discussion

The outlet temperature and the thermal efficiency of both the evacuated CPC solar collectors are presented in Figs. 6, 7, 8, 9 respectively. The most general equation used for the calculation of solar collector efficiency, which can be expressed as the ratio of the heat stored in the collector to the total heat amount incident onto the collector during the same time, is given by Eq.(3).

$$\eta = \frac{\dot{m}c_{\mathrm{p}}\left(T_{\mathrm{o,w}} - T_{\mathrm{i,w}}\right)}{AG} \tag{3}$$

Fig. 6 and Table 2 show that the test results of outlet temperatures of both two kinds of CPC solar collectors with their corresponding numerical calculation values. For both two solar collectors, the temperature deviations between the measured and calculated values are with less than 1% near identical. Therefore, it can be concluded that this result shows good agreement with experimental data, and the numerical model can accurately estimate the performance of solar collector.

Fig. 7 presents the measured outlet temperature of the different two solar collectors. The tracking CPC solar collector obtain higher outlet temperature than the stationary CPC solar collector due to the incident angle controlled by the tracking motor always tends to 0°. The temperature deviations at 12 (noon) presents the minimum value for the tracking CPC solar collector adjust to the exactly same position with the corresponding stationary CPC solar collector at that time. At the earlier/later time of 12 the temperature deviations are enlarged with increasing incident angle. These results are consistent with the ray-tracing calculation.

Table 4
Comparisons of thermal efficiency of stationary and tracking CPC solar collector with local time [%]

Local Time	Stationary-Exp [%]	Tracking-Exp [%]	(Tra. Eff.-Sta. Eff.)
8	22.88	56.07	33.19
9	26.60	54.42	27.82
10	46.28	52.77	6.49
11	49.44	52.37	2.93
12	51.39	51.73	0..34
13	51.71	53.22	1.51
14	49.99	54.10	4.11
15	38.64	57.34	18.70
16	20.23	59.56	39.33
Ave.	39.68	54.62	14.94

The thermal efficiencies of the stationary as well as the tracking CPC solar collector determined by numerical calculationand experiment measurement are shown in Fig. 8 and Table 3. The measured values show slightly higher than the numerical results. This is because the convective heat loss increases due to adopting a large convective heat loss coefficient for the calculation. As the incident angle increases, the thermal efficiency of the stationary CPC solar collector decreases. However, although the amount of absorbed heat for tracking CPC solar collector decreases with increasing incident angle, less heat loss accompanying with this process still make the thermal efficiency increase slightly. By considering the tracking mechanism errors, it can be concluded that the calculated results agree well with the measured results on the whole curves.

In Fig. 9 and Table 4, the efficiencies of stationary and tracking CPC solar collector determined by thermal method are presented. In a general view, the deviations between both solar collectors get enlarged as the incident angle increases due to the tracking effect. The absorbed heat amount of stationary CPC solar collector decreases sharply whereas the tracking CPC solar collector still maintains the normal incidence. The peak thermal efficiency of the stationary CPC solar collector denotes that irradiation is another deciding factor. The thermal efficiency of tracking CPC solar collector is up to 59.56% in this experiment and the average thermal efficiency of the tracking CPC solar collector is about 14.94% higher than that of the stationary CPC solar collector.

5. Conclusion

Two types of evacuated CPC (stationary and tracking) solar collectors are designed, manufactured and tested at outdoor field conditions. The thermal performances of stationary and tracking solar collector are investigated numerically and experimentally. In this study, the thermal efficiency is the effect with combination of both incident angle and the irradiation. More steadily changed thermal efficiency of tracking solar collector can be found easily due to the tracking effect. Tracking solar collector exceeded the stationary one in thermal efficiency of up to 14.94% because the tracking collector always adjusting the collector to face the sun for a normal incidence. One tolerance problem caused by the tracking system is due to the motor-driven mechanism moves exactly with the clock time instead of the real sun trace. The thermal resistant of the air between the inner glass and the copper tube will be high enough to reduce the convection heat exchange to some extend. It is still expected that this part of air could be eliminated though the glass tube have been sealed on both open ends in this research. Higher outlet temperatures will be available if the absorber diameter decreases to obtain higher geometrical concentration ratio. These consequences might be used for design or performance evaluation of the CPC solar collectors. The issues of the improvement of exact tracking and water loop design need further work.

References

[1] N.K. Abdul-Jabbar, S.A. Salman, Effect of two-axis sun tracking on the performance of compound parabolic concentrators, Energy Conversion and Management 39 (10) (1998) 1073–1079.
[2] M. Ronnelid, B. Perers, B. Karlsson, Construction and testing of a large-area CPC-collector and comparison with a flat plate collector, Solar Energy 57 (3) (1996) 177–184.
[3] Rene Tchinda, Nguijoi Ngos, A theoretical evaluation of the thermal performance of CPC with flat one-side absorber, International Communications in Heat and Mass transfer 33th, 2006, pp. 709–718.
[4] Yin Zhiqiang, Chinese all glass evacuated solar collector tubes during the past 18 years, Chinese Journal of Solar Energy 1 (1997).
[5] Q. Lin, S. Furbo, Solar heating systems with evacuated tubular solar collector, EuroSun 98 (1998) 1–7 III.2.27.
[6] Y. Tripanagnostopoulos, P. Yianoulis, S. Papaefthimiou, M. Souliotis, Th. Nousia, Cost effective asymmetric CPC solar collectors, Renewable Energy 16 (1999) 628–631.
[7] D.R. Mills, I.M. Bassett, G.H. Derrick, Relative cost-effectiveness of CPC reflector designs suitable for evacuated absorber tube solar collectors, Solar Energy 36 (3) (1986) 199–206.
[8] P. Gandhidasan, S. Satcunanathan, Energy collection augmentation in tracking flat plate collectors, Proceedings of Sun World Forum, Brighton, 1981, pp. 186–191.
[9] E. Papanicolaou, K. Voropoulos, V. Belesslotis, Natural convective heat transfer in an asymmetric greenhouse-type solar still — effect of angle of inclination, Numerical Heat Transfer 42 (8) (2002) 855–880.
[10] C. Lei, J.C. Patterson, Natural convection in a reservoir sidearm subject to solar radiation: a two-dimensional simulation, Numerical Heat Transfer 42 (1–2) (2002) 13–32.
[11] Trace Pro manual.
[12] J.A. Duffie, W.A. Beckman, Solar engineering of thermal processes, 2nd ed. John Wiley and Sons Inc, USA, 1991.
[13] D.K. Jo, Y.H. Kang, C.M. Auh, A study on the analysis of solar radiation characteristics on a high elevated area, Journal of the Korean Solar Energy Society 23 (3) (2003) 23–28.